CORTEX 80 (2016) 35–50

Available online at www.sciencedirect.com

ScienceDirect

Journal homepage: www.elsevier.com/locate/cortex

Special issue: Research report

# Visual adaptation provides objective electrophysiological evidence of facial identity discrimination

*Talia L. Retter** *and Bruno Rossion*

*Psychological Sciences Research Institute, Institute of Neuroscience, University of Louvain, Louvain-la-Neuve, Belgium*

ARTICLE INFO

*Article history:*
Received 17 July 2015
Reviewed 27 August 2015
Revised 29 October 2015
Accepted 23 November 2015
Published online 19 January 2016

*Keywords:*
Face perception
Adaptation
Identity discrimination
FPVS-EEG

ABSTRACT

Discrimination of facial identities is a fundamental function of the human brain that is challenging to examine with macroscopic measurements of neural activity, such as those obtained with functional magnetic resonance imaging (fMRI) and electroencephalography (EEG). Although visual adaptation or repetition suppression (RS) stimulation paradigms have been successfully implemented to this end with such recording techniques, objective evidence of an identity-specific discrimination response due to adaptation at the level of the visual representation is lacking. Here, we addressed this issue with fast periodic visual stimulation (FPVS) and EEG recording combined with a symmetry/asymmetry adaptation paradigm. Adaptation to one facial identity is induced through repeated presentation of that identity at a rate of 6 images per second (6 Hz) over 10 sec. Subsequently, this identity is presented in alternation with another facial identity (i.e., its anti-face, both faces being equidistant from an average face), producing an identity repetition rate of 3 Hz over a 20 sec testing sequence. A clear EEG response at 3 Hz is observed over the right occipito-temporal (ROT) cortex, indexing discrimination between the two facial identities in the absence of an explicit behavioral discrimination measure. This face identity discrimination occurs immediately after adaptation and disappears rapidly within 20 sec. Importantly, this 3 Hz response is not observed in a control condition without the single-identity 10 sec adaptation period. These results indicate that visual adaptation to a given facial identity produces an objective (i.e., at a pre-defined stimulation frequency) electrophysiological index of visual discrimination between that identity and another, and provides a unique behavior-free quantification of the effect of visual adaptation.



* *Corresponding author*. Institut de recherche en sciences psychologiques (IPSY), Université catholique de Louvain, 10 Place du Cardinal Mercier, 1348 Louvain-la-Neuve, Belgium.
E-mail addresses: talia.retter@uclouvain.be (T.L. Retter), bruno.rossion@uclouvain.be (B. Rossion).

http://dx.doi.org/10.1016/j.cortex.2015.11.025
0010-9452/

## 1. Introduction

The discrimination of facial identities serves as an important function for human social life and reflects the remarkable ability of the human visual system to distinguish between different exemplars within a category. This ability is especially impressive when considering that the physical differences between facial identities may be subtle and in the natural environment are often presented in tandem with dramatic differences in viewing conditions, e.g., luminance, direction of the lighting source, viewing angle, etc.

Despite the challenges in detecting relevant visual differences between facial identities and connecting such visual information to specific representations of these identities, humans are capable of discriminating images of facial identities rapidly and accurately (e.g., Jacques, d'Arripe, & Rossion, 2007). Further evidence that this function is specialized in the human brain comes from stimulus manipulations that uniquely affect discrimination of facial identities compared to discrimination within other object categories, e.g., the face inversion effect (Busigny & Rossion, 2010; Robbins & McKone, 2007; Rossion, 2008; Sergent, 1984; Valentine & Bruce, 1986; Yin, 1969 for review). Indeed, human face perception is known to implicate a complex, distributed network along the ventral surface of the occipito-temporal cortex with a right hemisphere advantage (e.g., Haxby, Hoffman, & Gobbini, 2000; Puce, Allison, Gore, & McCarthy, 1995; Rossion, Alonso-Prieto, Boremanse, Kuefner, & Van Belle, 2012; Rossion, Hanseeuw, & Dricot 2012; Sergent, Ohta, & MacDonald, 1992; Weiner & Grill-Spector, 2010; Zhen et al., 2015).

However, studying facial identity discrimination at a neural level has been challenging because measurements of macroscopic neural activity, such as those obtained with functional magnetic resonance imaging (fMRI), or electroencephalography (EEG), are not inherently sensitive to differences in facial identity. This is likely due to the level of organization at which face identity is coded in the brain. Recordings from macaque monkeys in the infero-temporal (IT) cortex have found single neurons that differentiate individual (human and monkey) facial identities, these neurons discharging at a different rates to pictures of different faces (e.g., Freiwald, Tsao, & Livingstone, 2009; Leopold, Bondar, & Giese, 2006; Rolls, 2001; Rolls, Aggelopoulos, Franco, & Treves, 2004; Young & Yamane, 1992). This has inspired the view that facial identities are coded for sparsely, i.e., within a small population of neurons. Therefore, if different facial identities are coded for with overlapping representations in a distributed neural population, differences in responses to facial identities may be revealed only at a very fine scale and may not be reflected in overall changes at the level of the population (Meyers, Borzello, Freiwald, & Tsao, 2015).

In humans, patterns of activity within regions have been used to examine finer-grained activations in fMRI [e.g., multivariate pattern analysis (MVPA); Kriegeskorte, Formisano, Sorger, & Goebel, 2007; Norman, Polyn, Detre, & Haxy, 2006]. However, approaches such as MVPA rely on the scale available from the voxel-resolution of fMRI (i.e., several cubic millimeters, an area containing millions of neurons), and there is no evidence that facial identity is coded on a corresponding scale. Hence, MVPA-fMRI has generally failed to decode (i.e., discriminate) face identity in cortical face-selective regions of the human brain (e.g., Kriegeskorte et al., 2007; Natu et al., 2010) or to provide evidence that such decoding is not based on low-level image cues differentiating a few items, without much reliability and consistency across studies (e.g., Gosaert & Op de Beeck, 2013; Nestor, Plaut, & Behrmann, 2011; see the discussion in Rossion, 2014; Dubois, de Berker, & Tsao, 2015; see however Davidesco et al., 2014 for discrimination of photographs of vastly different face identities in local field potential responses on the cortical surface). Given the limited spatial resolution of the technique, there is even less reason to expect that MVPA applied to EEG data measured on the scalp would be able to reliably distinguish neural responses to different facial identities.

Combining a visual paradigm of adaptation or repetition suppression (RS), namely, the reduction of neural activity following repetition of the same stimulus, to techniques such as fMRI and EEG has offered a reliable means to distinguish between neural representations of facial identities in the human brain. In humans, RS has been used from its first application with fMRI (fMR-A, Grill-Spector et al., 1999; Grill-Spector & Malach, 2001; Henson & Rugg, 2003) to define the regions subtending individual face discrimination (e.g., Andrews & Ewbank, 2004; Gauthier et al., 2000; Gentile & Rossion, 2014; Harris, Young, & Andrew, 2014) and characterize the nature of individual face discrimination in these regions (i.e., which properties or processes subtend individual face discrimination; see e.g., Andrews, Davies-Thompson, Kingstone, & Young, 2010; Davies-Thompson, Gouws, & Andrews, 2009; Ewbank & Andrews, 2008; Ewbank, Henson, Rowe, Stoyanova, & Calder, 2013; Goffaux, Schiltz, Mur, & Goebel, 2012; Grotheer, Hermann, Vidnyánszky, & Kovács, 2014; Jiang, Dricot, Blanz, Goebel, & Rossion, 2009; Schiltz & Rossion, 2006; Yovel & Kanwisher, 2005; Winston, Henson, Fine-Goulden, & Dolan, 2004).

Facial identity adaptation has also been used with human electrophysiology at the population level, i.e., EEG recorded on the scalp (see Engell & McCarthy, 2014, for evidence of RS of facial identity in electrocorticography). For instance, the N170, a negative component observed on occipito-temporal sites that is particularly large when evoked by faces (Bentin, McCarthy, Perez, Puce, & Allison, 1996; Rossion & Jacques, 2011 for review) is reduced in amplitude following the immediate repetition of a facial identity (e.g., Caharel, d'Arripe, Ramon, Jacques, & Rossion, 2009; Caharel, Collet, & Rossion, 2015; Caharel, Jiang, Blanz, & Rossion, 2009; Itier & Taylor, 2002; Heisz, Watter, & Shedden, 2006; Jacques et al., 2007). However, amplitude reduction of the N170 following face identity repetition is a relatively small effect compared to the overall amplitude of the N170, and may depend on specific stimulation parameters (i.e., immediate repetition, short interstimulus interval, long duration the face adapter; see Rossion & Jacques, 2011 for discussion). Therefore, the N170 adaptation effect requires many trials to reach statistical significance, and is not found systematically (e.g., Amihai, Deouell, & Bentin, 2012; Bindemann, Burton, Leuthold, & Schweinberger, 2008; Schweinberger, Pickering, Jentzsch, Burton, & Kaufmann,

2002). The effect of facial identity repetition is also observed at other time points, for instance, at the level of the early P1 component in some studies (e.g., Walther, Schweinberger, Kaiser, & Kovacs, 2013; Walther, Schweinberger, & Kovács, 2013), and, most notably, in an ERP modulation termed the N250r ("r" for repetition). The N250r peaks at 230–300 msec over occipito-temporal regions (Schweinberger, Huddy, & Burton, 2004; Schweinberger, Pfütze, & Sommer, 1995; Schweinberger et al., 2002; Tanaka, Curran, Porterfield, & Collins, 2006) and has been used in a number of studies to characterize facial identity adaptation (e.g., Bindemann et al., 2008; Schweinberger et al., 2002; Walther, Schweinberger, Kaiser, et al., 2013; Walther, Schweinberger, & Kovács, 2013). However, as with the N170, this effect is also relatively small; moreover, identification of the N250r, a relative difference rather than a component *per se*, is not straightforward (e.g., Faerber, Jürgen, & Schweinberger, 2015).

There are several other limitations of ERP adaptation studies for investigating facial identity discrimination. Due to the polarity of ERP components, it is difficult to define whether these effects reflect RS or enhancement: while the N170 is typically *reduced* in amplitude to repeated faces, the N250r corresponds to an *increase* of amplitude to repeated faces. This is problematic because these two effects cannot be directly combined in a single measure to quantify the magnitude of face identity adaptation at the population level. Moreover, one cannot exclude that these effects are driven by the superimposition of additional ERP components at these latencies. Thus, even though standard ERP recordings potentially provide useful information about the time course of face identity discrimination, characterizing the nature of face identity adaptation at the population level with this approach is extremely difficult, due to a lack of sensitivity, objectivity and direct quantification.

In the present study, we used human electrophysiology with an original visual stimulation technique aimed to 1) objectively define a visual discrimination response to individual facial exemplars with adaptation and 2) quantify this neural response at both the group and individual participant levels. Additionally, we sought to investigate the link between adaptation and the sharpening of individual face representation at the neural level. To this end, we applied EEG recording with an adaptation paradigm using fast periodic visual stimulation (FPVS).

An adaptation paradigm with FPVS allows for the objective definition of adaptation to one stimulus in contrast to another. This is possible because in FPVS, stimuli are presented at a fixed frequency and the EEG response is expected exactly at this frequency following frequency-domain analysis (so-called "steady-state visual evoked potentials", ssVEPs; Regan, 1989; see Norcia, Appelbaum, Ales, Cottereau, & Rossion, 2015 for general principles of the approach and a review[1]). Responses are also recorded with a high signal-to-noise ratio (SNR) in a recording time relatively short compared to standard ERP studies, including studies on individual face perception (Rossion, 2014; Rossion & Boremanse, 2011). Moreover, the SNR can be estimated directly by comparing the noise at neighboring frequencies to the target frequency (Meigen & Bach, 1999; Rossion, Alonso-Prieto, et al., 2012; Rossion, Hanseeuw, et al., 2012; Srinivasan, Russell, Edelman, & Tononi, 1999).

The adaptation paradigm used in the present study is a symmetry/asymmetry paradigm that, to our knowledge, has been previously used only in studies on direction-selectivity with motion adaptation (Ales & Norcia, 2009; Tyler & Kaitz, 1977). In its first application to high-level vision here, two face stimuli are presented in alternation at a fixed frequency of 6 Hz (F); this fast frequency is privileged because it provides enough time to individualize faces, but does not allow gaze exploration of the face (Alonso-Prieto, Van Belle, Liu-Shuang, Norcia, & Rossion, 2013; Gentile & Rossion, 2014). The 6 Hz presentation rate is expected to generate an EEG response exactly at 6 Hz. If these alternating stimuli are preceded by an adaption period to one of the stimuli, an asymmetry is produced in the response to the two stimuli. Therefore, a response is also expected at F/2, i.e., 3 Hz. The response at F/2 is thus separated from the response at the stimulation presentation frequency (F). It is specific to adaptation if it is not found or reduced in an unadapted condition.

This adaptation effect is present during the subsequent alternation of facial identities, such that the same testing sequences may be compared across adapted versus unadapted conditions, limiting confounds from testing conditions containing either a number of different facial identities or only one facial identity (Xu, Yue, Lescroart, Biederman, & Kim, 2009), as are typically used in adaptation paradigms with FPVS (Alonso-Prieto et al., 2013; Gentile & Rossion, 2014; Nemrodov, Jacques, & Rossion, 2015; Rossion, Alonso-Prieto, et al., 2012; Rossion & Boremanse, 2011; Rossion, Hanseeuw, et al., 2012; Vakli, Németh, Zimmer, & Kovács, 2014). Moreover, this adaptation response is generated without the need for participants to be aware of the experimental goals or to perform an explicit individual face discrimination task. The time-course of the adaptation effect may also be investigated over the duration of the testing sequence. Behaviorally, the dynamics of adaptation effects have been shown to be complex (see Webster & MacLeod, 2011) and influenced by the duration of adaptation and testing presentations (Leopold, Rhodes, Mueller, & Jeffery, 2015), although typically decaying rapidly and non-linearly (e.g., Rhodes, Jeffery, Clifford, & Leopold, 2007). Being able to examine adaptation effects with electrophysiology provides the advantage that these effects may be characterized across a continuous duration after an adaptation period (e.g., Kovács, Zimmer, Harza, & Vidnyánszky, 2007). In summary, by using an adaptation paradigm with FPVS and EEG recording, we sought to define and quantify adaptation

[1] The term "FPVS" is preferred here to the term "ssVEP" because FPVS refers to the approach rather than the type of EEG response expected (Rossion, 2014). Even though it is widely used, the term ssVEP is more ambiguous, since there are different definitions of what is a ssVEP as opposed to a standard ERP response (e.g., Heinrich, 2010; Norcia et al., 2015; Regan, 1982). Moreover, adaptation decreases the "steadiness" of the periodic EEG response (Nemrodov et al., 2015; Rossion & Boremanse, 2011), so that using the term ssVEP in the context of adaptation does not seem appropriate.

effects to individual facial identities in humans at the neural population level.

## 2. Materials and methods

### 2.1. Participants

Sixteen healthy participants (age range 20–30 years; five male), recruited from a university campus, were tested individually. They all reported normal or corrected-to-normal vision and were right-handed according to an adapted Edinburgh Handedness Inventory measurement (Oldfield, 1971). Additionally, they showed results in the normal range for face matching, according to the Benton Face Recognition Test (BFRT, scores ranged from 72 to 94% in accuracy; $M = 82\%$; $SE = 1.63$) (Benton & Van Allen, 1968). In exchange for time spent participating, they received monetary compensation. All participants gave signed, informed consent, before the beginning of the experiment, which was approved by the Biomedical Ethical Committee of the University of Louvain.

### 2.2. Stimuli

Face stimuli were prepared from seventy-two full-front photographs of Caucasian faces (half female) with neutral expressions. Adobe Photoshop CS5 was used to crop the faces to exclude external features, standardizing the faces by height (250 pixels), and equalizing mean pixel luminance (183/255). Using JPsychoMorph software (Tiddeman, 2005), three randomly selected faces of the same sex, each selected only once, were averaged together to make twenty-four novel identities. Then, all 12 female and 12 male face stimuli were averaged separately to create an average face for each sex of faces.

A pair of two facial identities was presented in each experimental trial; in total, eight of the twenty-four novel identities were used to create eight face pairs (Fig. 1). These pairs were designed to contain a somewhat standardized amount of physical difference between the two facial stimuli as follows. To create the second face in each pair, each face stimulus was morphed in terms of shape and texture through its average face towards its anti-face in a theoretical face space (e.g., Leopold, O'Toole, Vetter, & Blanz, 2001). Relative to the average face, each pair contained one face stimulus which was 80% the original identity and another face stimulus which was 80% its anti-face. Displayed on a monitor with an 1920 by 1080 pixel resolution from a distance of 80 cm, the stimuli subtended approximately 5.0 degrees of vertical visual angle at the original presentation size.

### 2.3. Procedure

The experiment was tested in a quiet, low-lit room of a university building. After taking informed consent, administering preliminary questionaires (about 15 min) and preparing the recording (about 30 min), the participant was seated in front of a computer monitor and computer keyboard. In total, the recording session for this experiment lasted for about 10–15 min. This time consisted of the presentation of 16 trials, each of which was about 34 sec in duration. There were about 10 sec in between trials and participants were offered a longer break halfway through the experiment.

During all stimulus presentation, the stimuli were shown at a constant rate of 6 images per second (6 Hz) by means of sinusoidal contrast modulation from 0 to 100% (Fig. 2A), using Psychtoolbox 3.0.9 for Windows (as used originally in Rossion & Boremanse, 2011), running over MATLAB R2009a (MathWorks, USA). Contrast was manipulated as a function of image properties: images were projected on a monitor with an applied gamma-correction verified by a photometer. Given a screen refresh rate of 120 Hz, the 6 Hz image presentation took 20 frames (i.e., 120 Hz/6 Hz) per complete image presentation cycle (i.e., from 0 to 100 to 0% contrast); the contrast at each frame corresponded to the percent contrast of the 6 Hz sinusoidal contrast function at that time.

When the two identities of a stimulus pair were presented alternatingly during the sequence, the identity repetition frequency was at 3 Hz (i.e., 6 Hz/2). At each stimulus presentation cycle the size of the image varied randomly across five steps between 90 and 110% of the original presentation size in order to reduce the potential impact of low-level adaptation (Dzhelyova & Rossion, 2014; Rossion & Boremanse, 2011). Participants' task was to attend to the images displayed on the

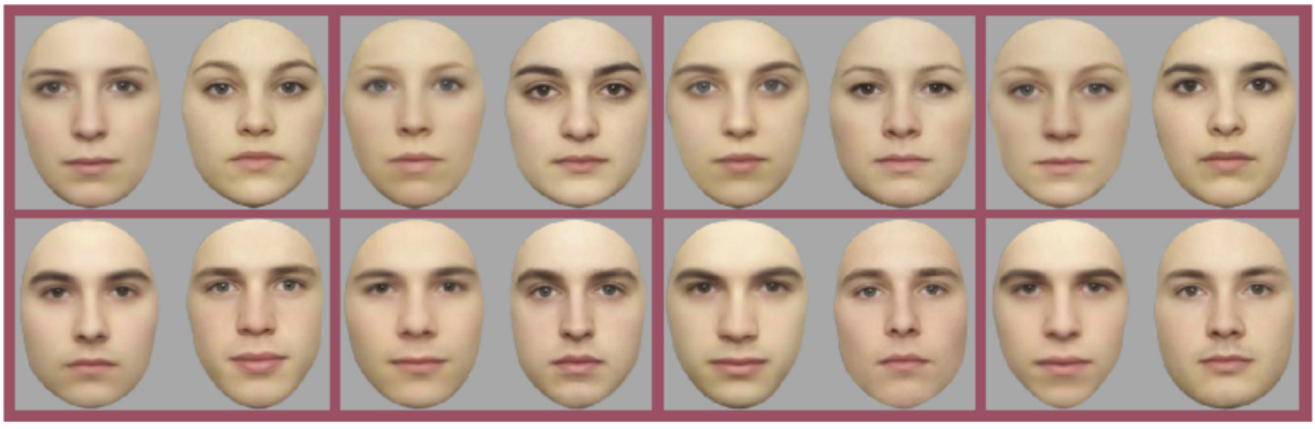

**Fig. 1 – The eight face/anti-face pairs used in the experiment.**

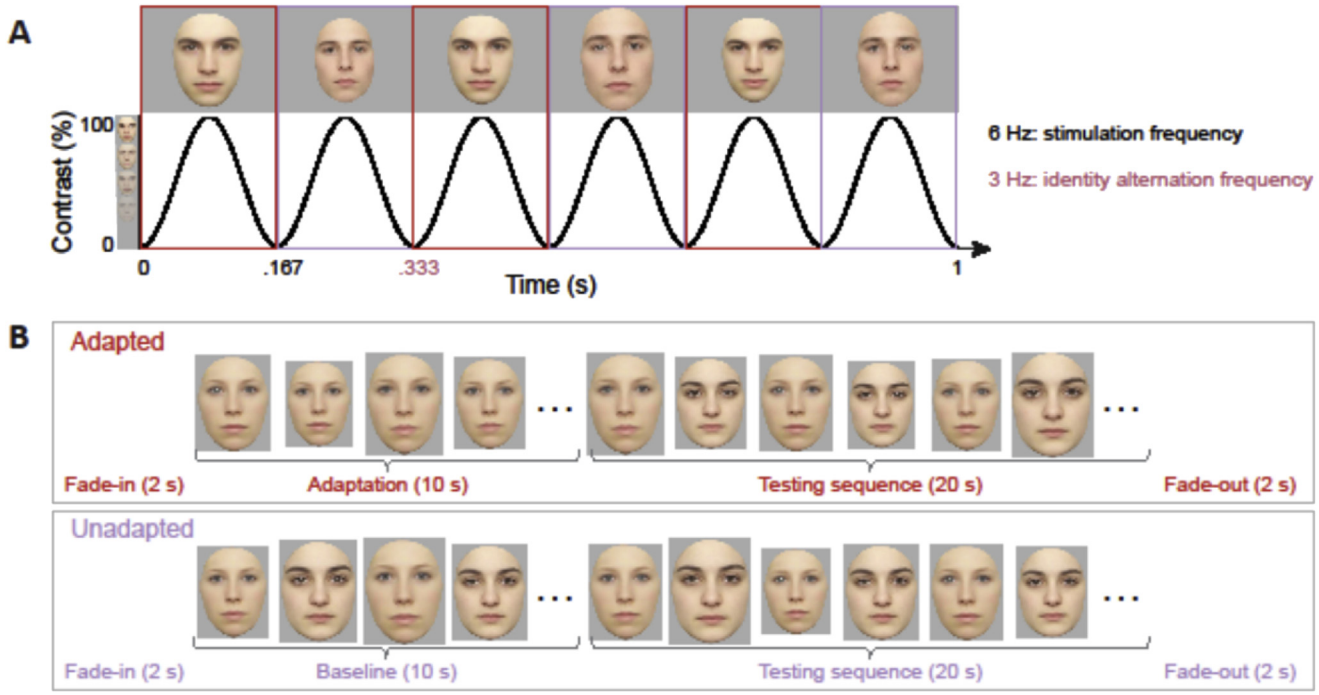


**Fig. 2 – A) Stimuli were presented through sinusoidal modulation from 0 to 100% contrast. An image was presented every 6 Hz, i.e., every .167 sec (1/6 Hz). When stimulus identity was alternated at each image presentation cycle, this alternation rate occurred at 3 Hz (i.e., 6 Hz/2, with a cycle length equivalent to 1/3 Hz = .333 sec). While the images depicting the amount of contrast on the y-axis occur in five steps for visualization here, during presentation this modulation occurred over about 10 steps, dictated by the screen refresh rate of 120 Hz. At each image presentation, the stimulus size varied between 90 and 110% of the original image presentation size. B) The two experimental conditions contained the same structure, except that in the "adapted" condition a single identity repeated in an adaptation baseline, while in the "unadapted" condition the stimulus identity alternated throughout the baseline duration as throughout the testing sequence.**

computer monitor while fixating on a centrally presented fixation cross, and to press on the space bar when that cross briefly changed color, which occurred four random times within each 34 sec trial.

In each experimental trial, only one pair of face/anti-face stimuli was presented. Each face pair was presented in only one type of experimental condition (counterbalanced across participants), in two repetitions: in one repetition with the face appearing first in the sequence and the other repetition with the anti-face appearing first. In the case that there was an adapting baseline, the adapting face always appeared first in the subsequent identity alternation.

There were two experimental conditions. In the *adapted* condition, the format of a trial was: 1) 2–5 sec of a grey background; 2) a 2 sec fade-in, during which the maximum stimulus contrast presentation gradually increased from zero to full contrast; 3) a 10 sec adaptation baseline, in which the same facial identity was presented repeatedly at the base frequency rate; 4) a 20 sec testing sequence, in which the adapting face was presented alternatingly with the other face in the stimulus pair; 5) a 2 sec graduate fade-out; 6) 2 of the grey background. In the *unadapted* condition, the 10 sec baseline instead contained an alternation of the two face stimuli, as in the testing sequence; otherwise, the trials were identical (Fig. 2B). Trial order was fully randomized for each participant.

In this paradigm, both low-level (e.g., luminance, contrast) and high-level (e.g., shape) responses are expected at the stimulus presentation rate, i.e., 6 Hz. This is the case when the same face stimulus is presented during the adaptation baseline, as well as during the alternation of the two face stimuli during the 20 sec sequence, if symmetrical responses are produced to each of the facial identities. However, if the adaptation baseline produces an adaptation effect (i.e., a difference in the response to the adapted face relative to the unadapted face) there is an expected *asymmetry* in the response at the rate of alternation, i.e., 3 Hz. Thus, the data will be examined during the 20 sec sequence, with the magnitude of the 3 Hz response indicating the spectral signature of adaptation (see Tyler & Kaitz, 1977; Figure 2 of Ales & Norcia, 2009).

### 2.4. *EEG acquisition*

The EEG data was recorded with a BioSemi ActiveTwo system, using 128 Ag–AgCl Active-electrodes, arranged in the default BioSemi configuration, which centers around nine standard 10/20 locations on the primary axes (BioSemi B.V., Amsterdam, Netherlands; for exact position coordinates, see http://www.biosemi.com/headcap.htm). Offsets of the electrodes, referenced to the common mode sense (CMS), were held below 40 mV. Additionally, four flat-type Active-electrodes were used

to record vertical and horizontal electrooculogram (EOG): two electrodes were placed above and below the participant's right eye and two were placed lateral to the external canthi. The EEG and EOG were digitized at a sampling rate of 512 Hz.

### 2.5. Analysis

The recorded EEG was analyzed using Letswave 5, an open source toolbox (http://nocions.webnode.com/letswave), running over MATLAB R2012b (MathWorks, USA).

#### 2.5.1. Preprocessing

After importation of the single data file of recorded EEG for each participant, changes in offset due to pauses in the recording in between trials were corrected for by aligning the offset for each channel at the start of a recording time to the offset prior to the pause. Next, the data was filtered: a fourth-order zero-phase Butterworth band-pass filter, with cutoff values of .1–120 Hz, was implemented, as well as a Fast Fourier Transform (FFT) multi-notch filter with a width of .5 Hz, used to remove electrical noise at three harmonics of 50 Hz. The data were then segmented by trial, including 1 sec before and after the time of stimulation. To correct for artifacts caused by blinks of the eyes, independent component analysis (ICA) with a square matrix was applied (Hyvarinen & Oja, 2000). A single component was removed only for two participants who blinked more than .2 times/s ($M = .08$, $SD = .09$) on average during the 30 sec stimulation sequences. Channels which were artifact-prone across multiple trials (0–3 channels per participant; less than 1% of channels on average) were linearly interpolated with pooled neighboring channels. All EEG channels were re-referenced to the common average.

#### 2.5.2. Frequency domain analysis

Each trial was re-segmented more precisely: starting after the baseline at the start of the 20 sec stimulation sequence up until an integer number of stimulation cycles of half the stimulus presentation frequency (3 Hz; i.e., until 19.7 sec). The trials were then averaged within each condition. Then, a FFT was computed in order to represent the data of each channel as a normalized amplitude spectrum (μV) in the frequency domain (range from 0 to 256 Hz), with a frequency resolution of .05 Hz (i.e., the inverse of the sequence length in seconds). For determining significance at the group level, the grand-averaged amplitude spectra were generated for each channel.

To quantify the response, three regions of interest (ROIs) were defined: medial occipital (MO), and right and left occipito-temporal (ROT and LOT, respectively) (e.g., Dzhelyova & Rossion, 2014). Each region was constituted of five channels: MO (PPOz, POz, POOz, Oz, and Oiz); ROT (PO10, P10, PO12, P8, PO8); and LOT (PO9, P9, PO11, P7, PO7). It was predicted that in both conditions low-level visual responses would be present at the stimulation frequency, i.e., 6 Hz, maximally at the MO ROI (Dzhelyova & Rossion, 2014; Liu-Shuang, Norcia, & Rossion, 2014); moreover, it was predicted that following adaptation, high-level, face-specific responses would also be present at the face alternation frequency, i.e., 3 Hz, maximally at the ROT ROI.

In order to determine when a significant response was present at the frequencies of interest and harmonics, Z-scores ($Z$ = (x-baseline)/standard deviation of the baseline) were computed across the ROIs of the grand-averaged amplitude spectra. Z-scores were computed with a baseline of the twenty bins surrounding the bin of interest (x), excluding the immediately adjacent bins (here, corresponding to a frequency range of about 1 Hz; e.g., Rossion, Alonso-Prieto, et al., 2012; Rossion, Hanseeuw, et al., 2012; Srinivasan, et al., 1999). A response was considered significant in a ROI if $Z > 2.32$, i.e., when $p < .01$. According to this criteria, the ROIs were also verified post-hoc: all of the MO channels individually gave a significant response at 6 Hz, and all the ROT channels individually gave a significant response at 3 Hz. So that the selection of these ROIs did not impair the detection of a response, analysis on the average of all EEG channels was also performed. Finally, to determine the range of significant harmonic responses to consider across conditions, the ROI with the maximal response overall was used to determine the highest significant harmonic frequency at which a significant response occurred.

To account for differences in baseline noise across the frequency spectrum, two separate methods of baseline-correction were applied to the individual participant data: a baseline-subtraction and a signal-to-noise (SNR) transform. The average of the twenty surrounding bins, excluding the immediately adjacent bin and the local maximum and minimum amplitude bins, was subtracted from the bin of interest in the former; in the latter (SNR), this average noise measurement was divided from the signal of interest (e.g., Rossion, Alonso-Prieto, et al., 2012; Rossion, Hanseeuw, et al., 2012). The baseline-subtraction was used for quantification of the response in microvolts, and the SNR was used for display of the response (e.g., Dzhelyova & Rossion, 2014). When responses were found at harmonics of the frequency of interest, the baseline-subtracted amplitudes of the harmonic responses were summed together (see Heinrich, 2009); note that, for the response at 3 Hz, the even harmonics were not considered, which corresponded with the general presentation rate of 6 Hz. Each channel of these baseline-corrected spectra was grand-averaged for display at the group level.

Statistical comparisons of the two experimental conditions were performed separately for the asymmetrical (3 Hz) and symmetrical (6 Hz and its harmonics) responses, given that an effect of adaptation is expected only at the asymmetrical response frequency, independently of the symmetrical response (Ales, Farzin, Rossion, & Norcia, 2012; Ales & Norcia, 2009; Liu-Shuang, Ales, Rossion, & Norcia, 2015a, 2015b). Comparisons were performed using two-way repeated measures ANOVAs, with factors of *Condition* (two levels: adapted and unadapted) and *Region* (three levels: MO, ROT, LOT). When Mauchly's test of sphericity was significant, a Greenhouse-Geisser correction was applied to the degrees of freedom.

#### 2.5.3. Temporal evolution in the frequency domain

Starting from the pre-processed data (re-referenced), the baseline and testing sequence were segmented into successive 5 sec segments in order to investigate the evolution of the adaptation response over time. Given previous evidence of

early face identity adaptation effects in EEG (e.g., Jacques et al., 2007; Nemrodov et al., 2015) and the rapid decay of behavioral face adaptation effects (e.g., Rhodes et al., 2007), we hypothesized that the adaptation effect would be concentrated in the beginning of the testing sequence following adaptation, although the duration of the adaptation and test delay time plays a role (Leopold et al., 2015) and long-term adaptation effects from minutes to hours have also been reported (Strobach & Carbon, 2013). This produced two segments in the baseline and four segments in the testing sequence. Segments were separately averaged within each condition and a FFT was applied to display data in the frequency domain with a frequency resolution of .20 Hz. A SNR baseline-correction was applied, with the noise defined as the six surrounding bins (a range of about 1.2 Hz), excluding the immediately adjacent bin and the local maximum and minimum amplitude bins. For display at the group level, each channel of the SNR spectra was grand-averaged. To determine significance of the response at each segment, Z-scores were computed exactly as described in the preceeding section except that, as in the SNR correction here, six surrounding bins were used to define the baseline. To enhance the temporal resolution, an additional analysis was performed as above, except with 2 sec segments and a baseline range of only two surrounding bins (for a similar range of 1.0 Hz).

#### 2.5.4. *Time-domain analysis*

Re-referenced data from preprocessing were more conservatively filtered with a fourth-order, zero-phase Butterworth low-pass filter, with a cutoff value of 30 Hz, as typically used in time-domain analyses of face-related ERPs (e.g., Jacques et al., 2007). The data were cropped precisely to the 20 sec testing sequence. Then, the data were segmented into 1 sec epochs, overlapping every two cycles (i.e., .33 sec); this led to 59 epochs per trial and 472 epochs per condition. These epochs were averaged by condition for each participant.

#### 2.5.5. *Behavioral data analysis*

To compare behavioral responses across conditions, paired-samples *t*-tests were used separately for accuracy and response time, with a two-tailed significance cutoff of $p < .05$. A correct response was indicated by a response on the space bar up to 1.5 sec following the time of the color change of the fixation cross. We additionally examined whether there was a correlation between the magnitude of the adaptation effect (baseline-subtracted amplitude over the maximal OT region for each participant) and the accuracy of the BFRT scoresby means of Pearson's correlation coefficient, with a significance cutoff of $p < .05$.

## 3. Results

### 3.1. *Effect of symmetry and assymetry (adaptation)*

#### 3.1.1. *Symmetrical responses (6 Hz)*

Symmetrical responses at the stimulation presentation frequency, i.e., 6 Hz, reflecting elements common to the response for each of the two alternatively presented facial identities, were present for both adapted and unadapted conditions (Fig. 3). As predicted, these responses were present maximally over the MO region in both conditions. An

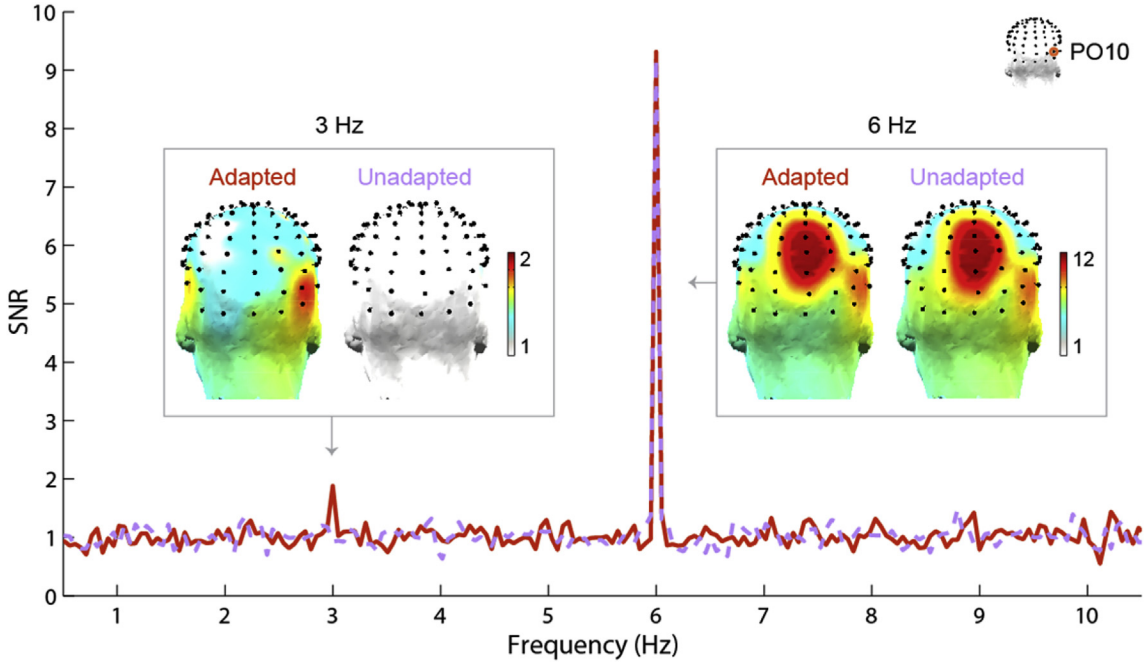


**Fig. 3 – Frequency-domain signal-to-noise (SNR) spectra of a single EEG channel (PO10, one of the channels in the ROT ROI; its location on the scalp is indicated by the topographical head above the spectrum) is shown. The topographies of the peak responses at 3 Hz and 6 Hz are shown above for both experimental conditions. The response at 6 Hz is present for both conditions, occurring maximally over the medial occipito-parietal region, while the response at 3 Hz is apparent only in the adapted condition, where it is maximal over the right occipito-temporal (ROT) region.**

average of all channels yielded significant responses for both condition at 6 Hz (adapted: $Z = 65.6$, $p < .001$; unadapted: $Z = 85.7$, $p < .001$) and its harmonics. At the MO ROI, five harmonics of this frequency produced significant responses (from 6 to 30 Hz) in each condition (for the first five harmonics, respectively: adapted: $Z = 102$, 35.7, 33.0, 9.67, and 4.87, all $p$'s $< .005$; unadapted: $Z = 86.9$, 27.0, 30.4, 11.1, 2.66, all $p$'s $< .005$). These harmonic responses were summed across each of the ROIs after a baseline-noise subtraction in order to quantify the response to the stimulation presentation frequency (Fig. 4A).

Statistical analyses revealed no significant effect of adaptation at the 6 Hz stimulation presentation frequency: there was no main effect of *Condition* (adapted or unadapted; $F_{1,15} = .611$; $p = .45$; $\eta_p^2 = .04$). There was a main effect of *ROI* ($F_{1.4,21} = 13.4$; $p = .001$; $\eta_p^2 = .47$), reflecting that the MO ROI produced the largest response, followed by the ROT and LOT ROIs in both conditions (Fig. 4A). However, there was no significant interaction between these two factors ($F_{2,14} = 1.51$; $p = .26$; $\eta_p^2 = .18$), indicating that there was no modulation of the region of activation by the testing condition.

#### 3.1.2. *Asymmetrical responses (3 Hz)*

It was predicted that following adaptation, high-level, asymmetrical responses would be present only at the face alternation frequency, i.e., 3 Hz. As predicted, these responses were present maximally over the ROT region, only in the adapted condition; no responses above noise-level were found in the unadapted condition at this frequency (Fig. 3). Analysis of the average of all EEG channels revealed a significant response only for the adapted condition (adapted: $Z = 1.83$, $p < .05$; unadapted: $Z = -.39$, $p > .05$). At the ROT ROI, only the first harmonic of this frequency produced a significant response in the adapted condition (at 3 Hz; $Z = 4.64$, $p < .001$). A quantification of the response at all ROIs revealed weaker responses at the LOT ROI and the MOI ROI for the adapted condition, and nearly no response for the unadapted condition at any of the ROIs (ROT ROI: $Z = .16$, $p > .05$) (Fig. 4B).

Statistical analyses revealed a significant effect of adaptation at the 3 Hz identity repetition frequency: there was a significant main effect of *Condition* (adapted or unadapted; $F_{1,15} = 11.6$; $p < .01$; $\eta_p^2 = .44$). There was no significant main effect of *ROI* ($F_{2,14} = 2.49$; $p = .12$; $\eta_p^2 = .26$). There was also no significant interaction between these two factors ($F_{2,14} = .981$; $p = .40$; $\eta_p^2 = .12$).

### 3.2. *Temporal evolution of the adaptation effect*

In order to investigate the duration of the adaptation effect present at 3 Hz in the adapted condition, the baseline and testing sequence were analyzed in 5-sec increments. The adaptation effect, i.e., the amplitude of the 3 Hz response, appears to be dramatically reduced beyond the first 5 sec following the adaptation baseline (Fig. 5). Z-scores computed separately at each segment revealed a significant response at 3 Hz only over these first 5 sec of the testing sequence at the ROT ROI, and only in the adapted condition ($Z = 3.03$, $p < .01$; all other $p$'s $> .05$). In contrast, at 6 Hz, a significant response was found at the MO ROI in every segment (all $p$'s $< .001$). Similar results were found in an additional analysis with 2-sec increments, providing a higher temporal resolution: Z-scores at 3 Hz revealed three significant contiguous responses for the adapted condition over the ROT ROI during the testing sequence, covering a range from 0 to 6 sec ($Z = 5.49$, 2.66, and 2.62, $p$'s $< .01$), as well as a non-contiguous significant response in the last 2 sec ($Z = 2.48$, $p < .01$).

### 3.3. *Time-domain signature of the adaptation effect*

The response at 3 Hz is thought to represent an asymmetry in the neural response to individual identities at the population level due to adaptation. To verify that this is the case, the data may also be examined in the time domain, at which asymmetries are expected to be found in the response to every other .167 sec face stimulus presentation cycle. This pattern of response is evident in the time domain (Fig. 6).

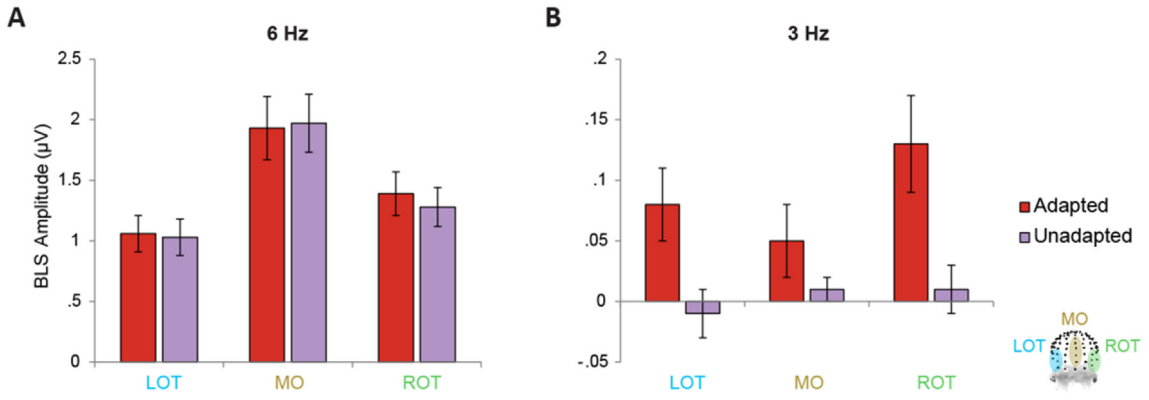


**Fig. 4 – Quantification of the responses at each of the three ROIs at the A) stimulation presentation frequency (6 Hz, here including the response at its four additional significant harmonics) and B) identity repetition frequency (3 Hz), for both the adapted and unadapted conditions. The mean response for the 16 participants is given in terms of baseline-subtracted amplitude (BLS Amplitude) with error bars representing one standard error above and below the mean.**

### 3.4. Behavioral results

There were no differences in responses (adapted accuracy: M = 96%, SE = 1.1%; unadapted accuracy: 96%, SE = 1.1%; adapted RT: M = 430 msec, SE = 71 msec; unadapted RT: M = 425 msec, SE = 17 msec) to the fixation-cross color change across conditions (accuracy: $t_{15} = .33$; $p = .75$, Cohen's $d = .08$; RT: $t_{15} = .97$; $p = .35$, Cohen's $d = .11$). No significant correlation between the amplitude of the adaptation effect was found with the BFRT scores ($r_{15} = .124$, $p = .65$).

## 4. Discussion

Alternating two facial identities at a fixed presentation rate of 6 Hz (i.e., 6 faces/sec) for 20 sec generated a response exactly at 6 Hz in the EEG spectrum, localized over the visual cortex. Most interestingly, neural adaptation to one of the two facial identities produced an additional response at the identity repetition rate of 3 Hz in the EEG spectrum. These results were discoverable thanks to the approach used here, FPVS in combination with EEG recording. As stated in the introduction, this FPVS-EEG approach has several strengths: 1) the amplitude of the response is defined in a single high-resolution frequency bin, thus *objectively* pre-determined by the chosen stimulation frequency; 2) the SNR is high, providing *sensitivity*; 3) *functionally specific* responses can be tagged with different stimulation presentation frequencies; here, an individual face discrimination response due to asymmetry following adaptation can be found at a separate frequency than the stimulus presentation frequency; 4) the response can be directly *quantified* as the amplitude (relative to noise level) in the two conditions, without having to deal with the complexity of opposite polarities of responses as in standard ERP measures; and 5) individual face discrimination is measured *without an explicit task*. Due to these advantages, an objective, sensitive, specific, and implicit response to individual face discrimination can be quantified.

### 4.1. A facial identity-specific discrimination response

FPVS has been used in two previous studies to study asymmetrical low-level (i.e., motion) EEG responses following adaptation (Ales & Norcia, 2009; Tyler & Kaitz, 1977). However, the response found here is unlikely to be accounted for by low-level visual information such as pixelwise differences in luminance or contrast between the two alternated images. Firstly, substantial random changes in size at each stimulus presentation were used. The presence of an adaptation effect in spite of low-level changes provides some evidence that this effect is, at least in part, occurring at high-level processing stages (e.g., Ewbank et al., 2013; see Dzhelyova & Rossion, 2014). Secondly, the response found here at 3 Hz peaked over the occipital-temporal cortex, rather than MO sites where low-level visual responses are localized in FPVS or low-level visual adaptation effects are typically found (e.g., Ales & Norcia, 2009), indicating that the response reflects contributions from high-level visual areas. Additionally, the 3 Hz response is maximal over the right hemisphere, 62% larger than the response over the left hemisphere; although this effect did not reach significance across regions ($p = .12$) due to the variability across individual participants although a right hemisphere lateralization supports a signature of processes that are involved specifically for faces (e.g., Hecaen & Angelergues, 1962; de Heering & Rossion, 2015; Hillger & Koenig, 1991; Sergent et al., 1992).

Finally, in the paradigm used here, the exact same testing sequences were analyzed across conditions, such that the

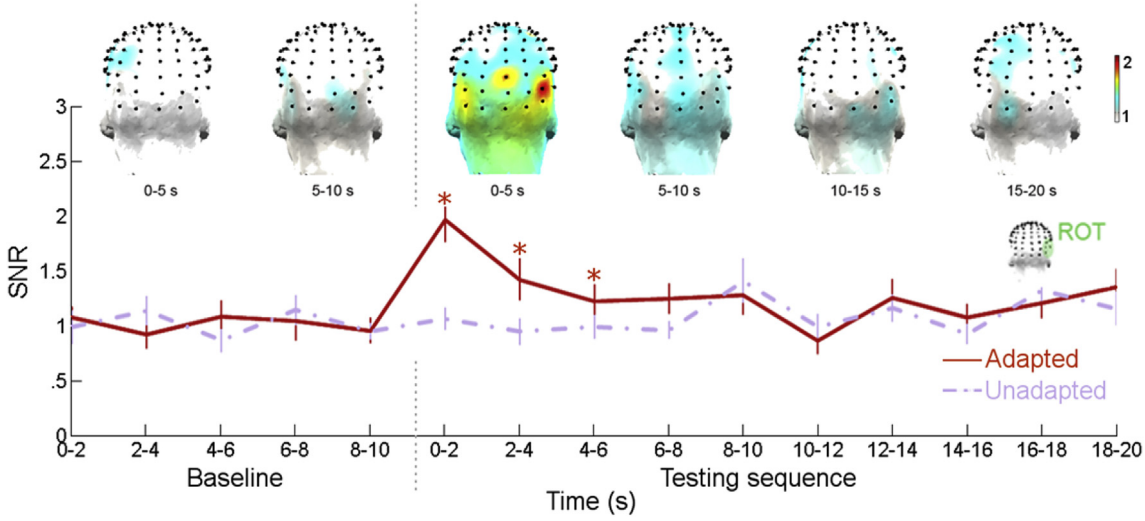


**Fig. 5 – The asymmetrical frequency-domain response at 3 Hz in the adaptation condition is plotted here in signal-to-noise ratio (SNR; noise-level = 1) as a function of the sequence over time. Each data point in the graph represents a non-overlapping 2 sec segment from the ROT ROI for the adapted (red) and unadapted (light purple) conditions; contiguous significant responses at 3 Hz ($Z > 2.32$, $p < .01$) are indicated by an asterisk. Error bars indicate one standard error above and below the mean. The topographical head plots each represent a 5 sec segment for the adapted condition: the first two plots depict the baseline period in which a single identity is repeated, while the testing sequence is shown in the four right head plots; all head plots are shown in SNR to a common scale (1–2).**

same information was present in both conditions during the testing sequence. This is unlike most adaptation designs with fMRI or EEG, including recent previous FPVS studies (e.g., Gentile & Rossion, 2014; Nemrodov et al., 2015; Rossion, Alonso-Prieto, et al., 2012; Rossion & Boremanse, 2011; Rossion, Hanseeuw, et al., 2012; Vakli et al., 2014), in which sequences containing repetitions of the same identity are contrasted to sequences containing a mixture of different identities.

Although selective attention is known to influence the magnitude of the response to FPVS (e.g., Müller et al., 2006; Norcia et al., 2015; Walter, Quigley, Andersen, & Mueller, 2012 for review), it is unlikely that attention produced the effect found here. Participants' task performance (i.e., detecting color changes of the centrally located fixation cross) did not vary across conditions. Note that a difference in attention between conditions would have changed the amplitude of the 6 Hz response, however, the 6 Hz response did not differ significantly between conditions and remained stable over time in our study. Most importantly, an attentional account of our effect is unlikely as it would require that participants synchronize precisely their attentional resources to the relatively fast rate at which the adapted and unadapted face alternate. Finally, stimulus pairs were presented in either the adapted or unadapted conditions within participants, such that adapting to a stimulus would not bias attention, or evoke effects of familiarity or long-term adaptation in a subsequent unadapted trial.

### 4.2. *The time-course of neural adaptation to facial identity*

Our results also showed that the adaptation effect was most pronounced within the first 2 sec after adaptation, after which the magnitude decreased quickly, becoming insignificant after 6 sec. This effect can be understood in the context of previous studies on the temporal dynamics of identity-specific adaptation effects. Behaviorally, identity aftereffects show an advantage for longer adapting and shorter testing times, with a power–law relationship associating these variables, similar to adaptation aftereffect dynamics for other types of visual stimuli (Leopold et al., 2015). However, the adapting and test phases may be separated by variable inter-stimulus intervals (ISIs), complicating a comparison of this relationship across studies (Strobach & Carbon, 2013). Here, two stimuli are presented in alternation without an explicit ISI, although due to the nature of the sinusoidal stimulus presentation (see Fig. 2), an ISI is simulated by

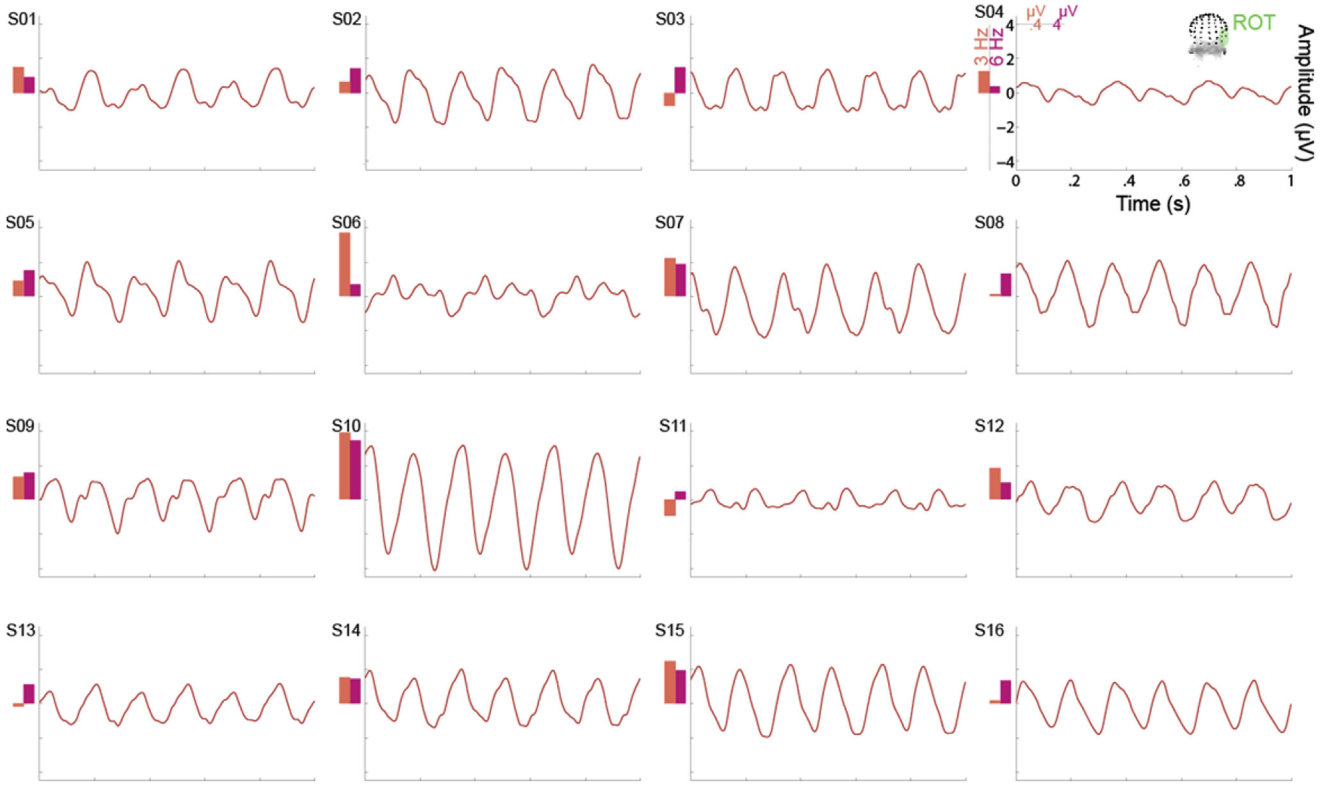


**Fig. 6 – Time-domain data from the ROT ROI for all sixteen individual participants in the adapted condition. The six cycles evident in 1 sec represent the response at 6 Hz in both conditions. Asymmetries are prominent every other cycle in the adapted condition, reflecting the enhanced identity discrimination response at 3 Hz. Note, however, that these asymmetries may be present in different forms (e.g., amplitude or phase) and are variable across participants (for this reason, data is not averaged across participants for display). The bars to the left of each time-domain plot indicate the quantified response for each participant at this ROI (see the group data in Fig. 4) at 3 Hz (orange; left) and 6 Hz (pink; right); with a y-axis placement corresponding to the zero of the time-domain plot; the different scales for these measures are indicated in the upper right figure.**

periods of low stimulus contrast (in between two stimulus presentations, each image is displayed at less than 50% contrast for half the stimulation cycle presentation duration, i.e., about 80 msec). However, the design here also makes comparison to other studies difficult, as the adapting stimulus continues to be displayed in alternation with an unadapted stimulus throughout the testing sequence. Nevertheless, the rapid, non-linear decay of the adaptation effect found here agrees with the rapid temporal dynamics of adaptation effects reported behaviorally (e.g., Rhodes et al., 2007), the early effects of face identity adaptation found on the N170 (e.g., Jacques et al., 2007; Rossion & Jacques, 2011 for review), or most recently with FPVS-EEG when identical faces are suddenly introduced after a long trains of different faces (Nemrodov et al., 2015).

### 4.3. *Potential neural mechanisms*

Besides providing objective evidence and direct quantification of facial identity adaptation in the human brain, we sought to use the results of this study to contribute to the understanding of the neural basis of identity-specific adaptation effects. For instance, Grill-Spector, Henson, and Martin (2006) suggested three mechanisms to potentially account for adaptation effects: fatigue, sharpening, and facilitation. *Fatigue* predicts the reduction of the response following adaptation as a result of decreased firing rates or synaptic efficacy of relevant neurons. Here, a decreased response to the adapted identity would creates an asymmetry because it would produce an alternation between large and small responses as the identities are alternated. *Sharpening* also predicts a reduced response for the adapted identity, since the response is made more specific as the response of neurons irrelevant to the representation is reduced. Here, sharpening and fatigue predict the same cause of asymmetry, i.e., a reduction of amplitude to the adapted identity, so that the present study cannot clarify this issue. However, time-domain representation and phase information could potentially give hints as to the underlying neural mechanisms of the adaptation response. For example, there is no direct evidence for fatigue or sharpening: there may be an increase in response amplitude to the unadapted identity as well as a decrease to the adapted identity (see Fig. 6). The third model, *facilitation*, predicts that there would be a decreased response latency or duration due to synaptic potentiation throughout the relevant neural network; here, this would be evidenced by a faster response to the adapted identity.

This facilitation account predicts that the effect will be expressed in terms of timing: effect of phase rather than or in addition to an effect of amplitude. Although EEG retains a high temporal resolution, absolute timing information may be masked in FPVS studies with rapid frequencies preventing a return to baseline activity in between stimulus presentations. Nevertheless, differences in phase, reflecting relative differences in timing, have been found between conditions using this technique (e.g., Appelbaum & Norcia, 2009; Cottereau, McKee, Ales, & Norcia, 2011; Rossion, Alonso-Prieto, et al., 2012; Rossion & Boremanse, 2011; Rossion, Hanseeuw, et al., 2012). Additionally, even though in the study of Rossion and Boremanse (2011), different (unadapting) and identical (adapting) face presentations were not described as showing a difference in phase, such effects may have been present in some participants (see Fig. 7). Here, differences in timing and/or amplitude following adaptation could be expected to produce responses at F/2 (3 Hz), and we aimed to investigate the nature of these differences.

However, although differences in both amplitude and phase are apparent visually (Fig. 6), we did not have a way to dissociate these response components. In this experiment, the lack of a response at 3 Hz (and so a lack of meaningful phase information at 3 Hz) in the unadapted condition prevents a comparison within participants of the phase shift of adaptation, so that timing estimates cannot be made from the phase here. Additionally, variability in phase shifts in response to individual stimulus pairs limits a comparison of adapted and unadapted conditions within participants in the present design. However, to further investigate the effect of adaptation on the phase of the response, we may investigate the variability of phase across participants at both 3 and 6 Hz: since the response at 3 Hz reflects the difference in the response to the two faces of the stimulus pair, this value should be somewhat consistent across participants; the variability in phase at 6 Hz is used as a very approximate reference. This analysis reveals that, indeed, phase appears randomly distributed at 3 Hz without adaptation, while the variability in phase at 3 Hz across participants is more comparable to that at 6 Hz (Fig. 7). Additionally, it can be seen that responses of larger magnitude are more related in phase, although this could be taken as indication that the phase estimate is more reliable in this case as well as that participants who show a larger adaptation effect in terms of amplitude also show a larger adaptation effect in terms of phase.

### 4.4. *Interpretations from FPVS-EEG*

Although the symmetry/asymmetry FPVS approach has been validated to study adaptation (Ales & Norcia, 2009; Tyler & Kaitz, 1977), this is not to say that the approach does not depart from other traditional adaptation paradigms, and the results found here should be interpreted in light of some of these differences. One aspect to consider is that the use of FPVS necessitates the choice of presenting stimuli at a specific frequency. However, although the frequency of stimulation is known to affect the measurement of individual face discrimination, the stimulation frequency may be chosen to match the optimal rate of the system for the process being measured: for this reason, 6 Hz was used as the stimulation presentation frequency (Alonso-Prieto et al., 2013; Gentile & Rossion, 2014). Stimulation frequencies may be understood in the context of the temporal distance between stimulus presentations: here, stimuli were presented every 167 msec, and alternated every 333 msec, a time window large enough to capture differences in the response to different facial identities (e.g., Jacques & Rossion, 2006; Walther, Schweinberger, Kaiser, et al., 2013). Additionally, at this rate only a single gaze fixation may be made, allowing for a measurement uncontaminated by eye movements at each presentation cycle and corresponding to the minimal amount of time necessary to identify faces at maximal performance (Hsiao & Cottrell, 2008) or reduce interindividual variance in the extraction of social information from faces to its minimum (Todorov, Pakrashi, &

Oosterhof, 2009; Willis & Todorov, 2006). Still, there is likely a viable range of stimulation frequencies which may have been used in this study; while different frequencies in this range may have be optimal for measuring a discrimination response here, this is likely to affect the magnitude of the response rather than its presence.

### 4.5. *A powerful approach to characterize facial identity representation*

Overall, the present paradigm, which is used to test high-level functions for the first time to our knowledge, may be particularly informative for studying adaptation and identity-specific representation at a neural level, and at the least it may provide a platform for futures studies on facial adaptation effects. For instance, one could easily test whether a 3 Hz asymmetrical response emerges or increases in this paradigm following adaptation with one of the identity presented under a different view than at test (e.g., a profile face as an adaptor followed by an alternation of full front faces), allowing measurement and characterization of generalization or invariance of face-identity adaptation (such as reported behaviorally: e.g., Jiang, Blanz, & O'Toole, 2006; or on the N170: Caharel, d'Arripe, Ramon, Jacques, & Rossion, 2009; Caharel, Jiang, Blanz, & Rossion, 2009; Caharel, Jacques, d'Arripe, Ramon, & Rossion, 2011; Caharel et al., 2015).

The paradigm also provides a unique way to address an outstanding issue in face processing: why behavioral performance at matching different views of familiar faces is significantly better than for unfamiliar faces (Megreya & Burton, 2006; Young, Hay, McWeeny, Flude, & Ellis, 1985). Although such behavioral findings have generally been taken as evidence that familiar and unfamiliar faces are processed by qualitatively different representations (Balas, Cox, & Conwell,

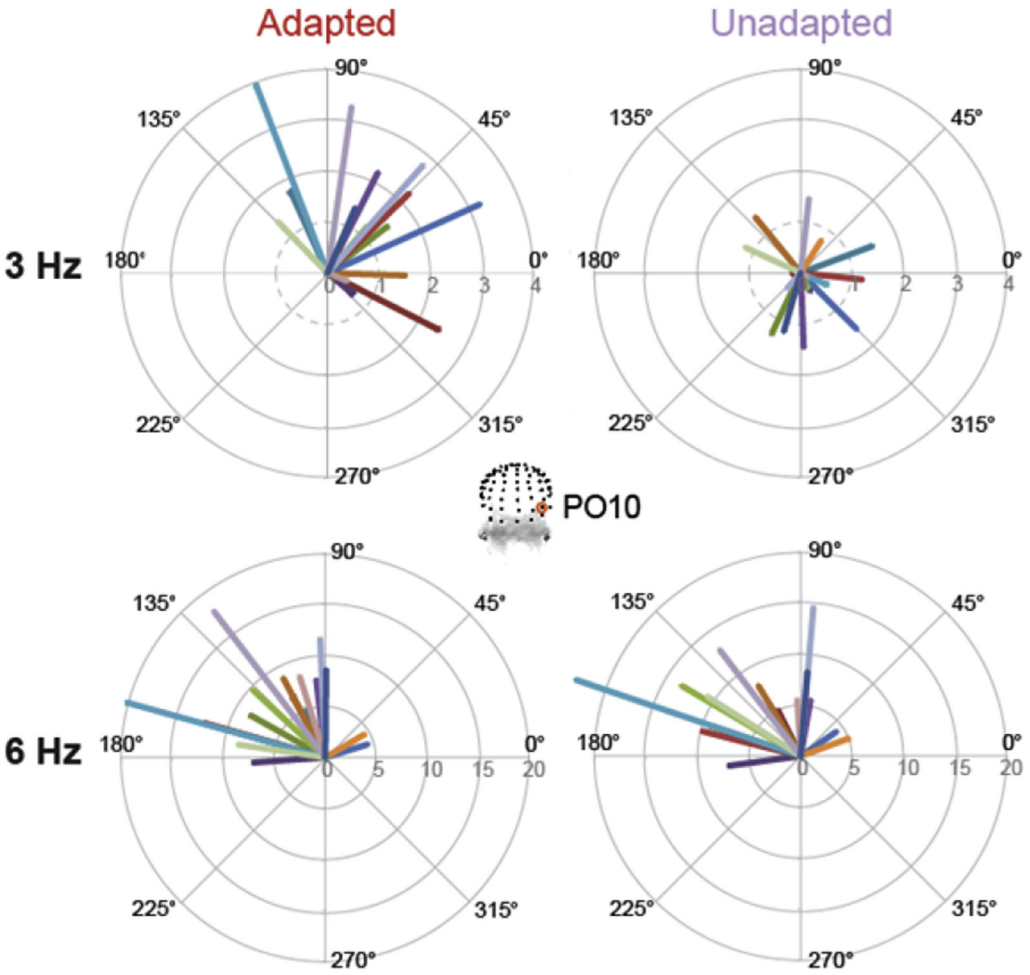


**Fig. 7 – The phase at the ROT channel PO10 is plotted from 0 to 360° for each of the individual participants, with the length of the vector representing the SNR of the response at that channel (noise level = 1). In the bottom row, the response at the stimulation presentation frequency, 6 Hz, indicates the amount of variability across participants and conditions when a similar response with a large SNR is recorded. In the top row, at 3 Hz, there is a similar amount of variability within the adapted condition (although, note that the temporal duration indicated by degree measurements is relative to the frequency: 1° of a 3 Hz cycle represents .93 msec, while 1° of a 6 Hz cycle represents .46 msec); in contrast, when no significant response is recorded at the group level in the unadapted condition, the phase values appear randomly distributed. Note that the scale of the SNR along the concentric circles is matched within each row but varies across the two rows.**

2007; Carbon, 2008; Gobbini et al., 2013; Knappmeyer, Thornton, & Bülthoff, 2003; Megreya & Burton, 2006; Tong & Nakayama, 1999; Visconti di Oleggio Castello, Guntupalli, Yang, & Gobbini, 2014; Watier & Collin, 2009), behavioral measures cannot disentangle the multiple levels of representations that can be used to match different pictures of familiar faces as compared to unfamiliar faces: not only visual but also semantic and verbal representations (e.g., Jenkins, White, Van Montfort, & Burton, 2011; i.e., matching two different pictures of a well-known familiar individual may not be performed by comparing the visual stimuli but associating each of these pictures with the same name, something that cannot be done for unfamiliar faces). In contrast, in the present EEG paradigm measuring an implicit response over the visual cortex, a greater increase in the 3 Hz response for familiar than unfamiliar faces would provide unambiguous evidence that familiar faces are more distinct than unfamiliar faces at the level of visual representations.

This example leads to a major implication of these observations: that this FPVS-EEG paradigm may be applied to provide an alternative to a behavioral discrimination task, which may be biased by a number of external factors. Here, since the response is recorded from participants who are not asked to perform a task related to the identity of the faces presented, the response measured is an implicit one. Thus, this approach may aid in resolving the inconsistent finding of an enhancement in discrimination ability in previous adaptation studies with behavioral measures (see Oruc & Barton, 2011; Webster & MacLeod, 2011). A further implication is that the task could be used with participants unable to give a reliable behavioral response, such as infants, young children, or patient populations. Thus, this adaptation paradigm with FPVS-EEG may provide a tool for further investigation of facial identity or other contrast responses between two high-level visual stimuli.

## Acknowledgments

TR is supported by the Belgian National Fund for Scientific Research (Fonds de la Recherche Scientifique; FNRS:FC7159). This work was also supported by a grant from the European Research Council (ERC: facessvep 284025) to BR. We would like to thank Renaud Laguesse for preparing the original face photographs and Milena Dzhelyova for her help with creating the face/anti-face stimulus pairs.

## REFERENCES

Ales, J. M., Farzin, F., Rossion, B., & Norcia, A. M. (2012). An objective method for measuring face detection thresholds using the sweep steady-state visual evoked response. *Journal of Vision, 12*(10), 1–18.

Ales, J. M., & Norcia, A. M. (2009). Assessing direction-specific adaptation using the steady-state visual evoked potential: results from EEG source imaging. *Journal of Vision, 9*(7), 1–13.

Alonso-Prieto, E. A., Van Belle, G., Liu-Shuang, J., Norcia, A. M., & Rossion, B. (2013). The 6Hz fundamental frequency rate for individual face discrimination in the right occipito-temporal cortex. *Neuropsychologia, 51*, 2863–2975.

Amihai, I., Deouell, L. Y., & Bentin, S. (2012). Neural adaptation is related to face repetition irrespective of identity: a reappraisal of the N170 effect. *Experimental Brain Research, 209*(2), 193–204.

Andrews, T. J., Davies-Thompson, J., Kingstone, A., & Young, A. W. (2010). Internal and external features of the face are represented holistically in face-selective regions of visual cortex. *Journal of Neuroscience, 30*(9), 3544–3552.

Andrews, T. J., & Ewbank, M. P. (2004). Distinct representations for facial identity and changeable aspects of faces in the human temporal lobe. *NeuroImage, 23*, 905–913.

Appelbaum, L. G., & Norcia, A. M. (2009). Attentive and pre-attentive aspects of figural processing. *Journal of Vision, 9*(11), 1–12.

Balas, B., Cox, D., & Conwell, E. (2007). The effect of real-world personal familiarity on the speed of face information processing. *PLoS One, 2*(11), e1223.

Bentin, S., McCarthy, G., Perez, E., Puce, A., & Allison, T. (1996). Electrophysiological studies of face perception in humans. *Journal of Cognitive Neuroscience, 8*, 551–565.

Benton, A. L., & Van Allen, M. W. (1968). Prosopagnosia and facial discrimination. *Journal of the Neurological Sciences, 15*, 167–172.

Bindemann, M., Burton, A. M., Leuthold, H., & Schweinberger, S. R. (2008). Brain potential correlates of face recognition: geometric distortions and the N250r brain response to stimulus repetitions. *Psychphysiology, 45*(4), 535–544.

Busigny, T., & Rossion, B. (2010). Acquired prosopagnosia abolishes the face inversion effect. *Cortex, 46*, 965–981. Read more: http://face-categorization-lab.webnode.com/publications/.

Caharel, S., d'Arripe, O., Ramon, M., Jacques, C., & Rossion, B. (2009). Early adaptation to unfamiliar faces across viewpoint changes in the right hemisphere: evidence from the N170 ERP component. *Neuropsychologia, 47*, 639–643.

Caharel, S., Collet, K., & Rossion, B. (2015). The early visual encoding of a face (N170) is viewpoint-dependent: a parametric ERP-adaptation study. *Biological Psychology, 106*, 18–27.

Caharel, S., Jacques, C., d'Arripe, O., Ramon, M., & Rossion, B. (2011). Early electrophysiological correlates of adaptation to personally familiar and unfamiliar faces across viewpoint changes. *Brain Research, 1387*, 85–98.

Caharel, S., Jiang, F., Blanz, V., & Rossion, B. (2009). Recognizing an individual face: 3D shape contributes earlier than 2D surface reflectance information. *NeuroImage, 47*, 1809–1818.

Carbon, C. C. (2008). Famous faces as icons. The illusion of being an expert in the recognition of famous faces. *Perception, 2008*(37), 801–806.

Cottereau, B. R., McKee, S. P., Ales, J. M., & Norcia, A. M. (2011). Disparity-tuned population responses from human visual cortex. *Journal of Neuroscience, 31*(3), 954–965.

Davidesco, I., Zion-Golumbic, E., Bickel, S., Harel, M., Groppe, D. M., Keller, C. J., et al. (2014). Exemplar selectivity reflects perceptual similarities in the human fusiform cortex. *Cerebral Cortex, 24*, 1879–1893.

Davies-Thompson, J., Gouws, A., & Andrews, T. J. (2009). An image-dependent representation of familiar and unfamiliar faces in the human ventral stream. *Neuropsychologia, 47*, 1627–1635.

Dubois, J., de Berker, A. O., & Tsao, D. Y. (2015). Single-unit recordings in the macaque face patch system reveal limitations of fMRI MVPA. *Journal of Neuroscience, 35*(6), 2791–2802.

Dzhelyova, M., & Rossion, B. (2014). The effect of parametric stimulus size variation on individual face discrimination indexed by fast periodic visual stimulation. *BMC Neuroscience, 15*(87), 1–12.

Engell, A. D., & McCarthy, G. (2014). Repetition suppression of face-selective evoked and induced EEG recorded from human cortex. *Human Brain Mapping, 35*, 4155–4162.

Ewbank, M. P., & Andrews, T. J. (2008). Differential sensitivity for viewpoint between familiar and unfamiliar faces in human visual cortex. *NeuroImage, 40*, 1857–1870.
Ewbank, M. P., Henson, R. N., Rowe, J. B., Stoyanova, R. S., & Calder, A. J. (2013). Different neural mechanisms within occipitotemporal cortex underlie repetition suppression across same and different-size faces. *Cerebral Cortex, 23*, 1073–1084.
Faerber, S. J., Jürgen, M. K., & Schweinberger, S. R. (2015). Early temporal negativity is sensitive to perceived (rather than physical) facial identity. *Neurospcyologia, 75*, 132–142.
Freiwald, W. A., Tsao, D. Y., & Livingstone, M. S. (2009). A face feature space in the macaque temporal lobe. *Nature Neuroscience, 12*(9), 1187–1196.
Gauthier, I., Tarr, M. J., Moylan, J., Skudlarski, P., Gore, J. C., & Anderson, A. W. (2000). The fusiform "face area" is part of a network that processes faces at the individual level. *Journal of Cognitive Neuroscience, 12*(3), 495–504.
Gentile, F., & Rossion, B. (2014). Temporal frequency tuning of cortical face-sensitive areas for individual face perception. *NeuroImage, 90*, 256–265.
Gobbini, M. I., Gors, J. D., Halchenko, Y. O., Rogers, C., Guntupalli, J. S., Hughes, H., et al. (2013). Prioritized detection of personally familiar faces. *PLoS One, 8*(6), e66620.
Goffaux, V., Schiltz, C., Mur, M., & Goebel, R. (2012). Local discriminability determines the strength of holistic processing for faces in the fusiform face area. *Frontiers in Psychology, 3*, 604.
Gosaert, E., & Op de Beeck, H. P. (2013). Representations of facial identity information in the ventral visual stream investigated with multivoxel pattern analyses. *Journal of Neuroscience, 33*(19), 8549–8558.
Grill-Spector, K., Henson, R., & Martin, A. (2006). Repetition and the brain: neural models of stimulus-specific effects. *Trends in Cognitive Sciences, 10*(1), 14–23.
Grill-Spector, K., Kushnir, T., Edelman, S., Avidan, G., Itzchak, Y., & Malach, R. (1999). Differential processing of objects under various viewing conditions in the human lateral occipital complex. *Neuron, 24*(1), 187–203.
Grill-Spector, K., & Malach, R. (2001). fMR-adaptation: a tool for studying the functional properties of human cortical neurons. *Acta Psychologica, 107*, 293–321.
Grotheer, M., Hermann, P., Vidnyánszky, Z., & Kovács, G. (2014). Repetition probability effects for inverted faces. *NeuroImage, 102*(2), 416–423.
Harris, R. J., Young, A. W., & Andrew, T. J. (2014). Brain regions involved in processing facial identity and expression are differentially selective for surface and edge information. *NeuroImage, 97*(100), 217–223.
Haxby, J. V., Hoffman, E. A., & Gobbini, M. I. (2000). The distributed human neural system for face perception. *Trends in Cognitive Science, 4*, 223–233.
Hecaen, H., & Angelergues, R. (1962). Agnosia for faces (prosopagnosia). *Archives of Neurology, 7*, 92–100.
de Heering, A., & Rossion, B. (2015). Rapid categorization of natural face images in the infant right hemisphere. *eLife, 4*. e06564, 1–14.
Heinrich, S. P. (2009). Permutation-based significance tests for multiharmonic steady-state evoked potentials. *IEEE Transactions on Biomedical Engineering, 56*(2), 534–537.
Heinrich, S. P. (2010). Some thoughts on the interpretation of steady-state evoked potentials. *Documenta Ophthalmology, 120*, 205–214.
Heisz, J. J., Watter, S., & Shedden, J. M. (2006). Automatic face identity encoding at the N170. *Vision Research, 46*(28), 4604–4614.
Henson, R. N. A., & Rugg, M. D. (2003). Neural response suppression, haemodynamic repetition effects, and behavioural priming. *Neuropsychologia, 41*, 263–270.
Hillger, L. A., & Koenig, O. (1991). Separable mechanisms in face processing: evidence from hemispheric specialization. *Journal of Cognitive Neuroscience, 3*, 42–58.
Hsiao, J. H., & Cottrell, G. (2008). Two fixations suffice in face recognition. *Psychological Science, 19*, 998–1006.
Hyvarinen, A., & Oja, E. (2000). Independent component analysis: algorithms and applications. *Neural Networks, 13*, 411–430.
Itier, R. J., & Taylor, M. J. (2002). Inversion and contrast polarity reversal affect both encoding and recognition processes of unfamiliar faces: a repetition study using ERPs. *NeuroImage, 15*, 353–372.
Jacques, C., d'Arripe, O., & Rossion, B. (2007). The time course of the inversion effect during individual face discrimination. *Journal of Vision, 7*(8), 1–9.
Jacques, C., & Rossion, B. (2006). The speed of individual face categorization. *Psychological Science, 17*, 485–492.
Jenkins, R., White, D., Van Montfort, X., & Burton, A. M. (2011). Variability in photos of the same face. *Cognition, 121*(3), 313–323.
Jiang, F., Blanz, V., & O'Toole, A. J. (2006). Probing the visual representation of faces with adaptation: a view from the other side of the mean. *Psychological Science, 17*(6), 493–500.
Jiang, F., Dricot, L., Blanz, V., Goebel, R., & Rossion, B. (2009). Neural correlates of shape and surface reflectance information in individual faces. *Neuroscience, 163*, 1078–1091.
Knappmeyer, B., Thornton, I. M., & Bülthoff, H. H. (2003). The use of facial motion and facial form during the processing of identity. *Vision Research, 43*, 1921–1936.
Kovács, G., Zimmer, M., Harza, I., & Vidnyánszky, Z. (2007). Adaptation duration affects the spatial selectivity of facial aftereffects. *Vision Research, 47*(25), 3141–3149.
Kriegeskorte, N., Formisano, E., Sorger, B., & Goebel, R. (2007). Individual faces elicit distinct response patterns in human anterior temporal cortex. *Proceedings of the National Academy of Sciences, 105*(51), 20600–20605.
Leopold, D. A., Bondar, I. V., & Giese, M. A. (2006). Norm-based face encoding by single neurons in monkey inferotemporal cortex. *Nature, 442*, 572–575.
Leopold, D. A., O'Toole, A. J., Vetter, T., & Blanz, V. (2001). Prototype-referenced shape encoding revealed by highlevel aftereffects. *Nature Neuroscience, 4*, 89–94.
Leopold, D. A., Rhodes, G., Mueller, K., & Jeffery, L. (2015). The dynamics of visual adaptation to faces. *Philosophical Transactions of the Royal Society of London B, 272*, 897–904.
Liu-Shuang, J., Ales, J. M., Rossion, B., & Norcia, A. M. (2015a). The effect of contrast polarity reversal on face detection: evidence of perceptual asymmetry from sweep VEP. *Vision Research, 108*, 8–19.
Liu-Shuang, J., Ales, J. M., Rossion, B., & Norcia, A. M. (2015b). Separable effects of inversion and contrast reversal on face detection thresholds and response functions: a sweep VEP study. *Journal of Vision, 15*(2).
Liu-Shuang, J., Norcia, A. M., & Rossion, B. (2014). An objective index of individual face discrimination in the right occipito-temporal cortex by means of fast periodic visual stimulation. *Neuropsychologia, 52*, 57–72.
Megreya, A. M., & Burton, A. M. (2006). Unfamiliar faces are not faces: evidence from a matching task. *Memory & Cognition, 34*, 865–876.
Meigen, T., & Bach, M. (1999). On the statistical significance of electrophysiological steady-state responses. *Documenta Ophthalmology, 98*, 207–232.
Meyers, E. M., Borzello, M., Freiwald, W. A., & Tsao, D. (2015). Intelligent information loss: the coding of facial identity, head pose, and non-face information in the macaque face patch system. *Journal of Neuroscience, 35*(18), 7069–7081.
Müller, M. M., Andersen, S., Trujillo, N. J., Valdes-Sosa, P., Malinowski, P., & Hillyard, S. A. (2006). Feature-selective attention enhances color signals in early visual areas of the

human brain. *Proceedings of the National Academy of Sciences, 103*(38), 14250–14254.
Natu, V. S., Jiang, F., Narvekar, A., Keshvari, S., Blanz, V., & O'Toole, A. J. (2010). Dissociable neural patterns of facial identity across changes in viewpoint. *Journal of Cognitive Neuroscience, 22*(7), 1570–1582.
Nemrodov, D., Jacques, C., & Rossion, B. (2015). The temporal dynamics of periodic electrophysiological responses to face-identity adaptation. *International Journey of Psychophysiology, 98*(1), 35–43.
Nestor, A., Plaut, D. C., & Behrmann, M. (2011). Unraveling the distributed neural code of facial identity through spatiotemporal pattern analysis. *Proceedings of the Natural Academy of Sciences of the United States of America, 108*, 9998–10003.
Norcia, A. M., Appelbaum, L. G., Ales, J. M., Cottereau, B., & Rossion, B. (2015). The steady-state visual evoked potential in vision research: a review. *Journal of Vision, 15*(6)(4), 1–46.
Norman, K. A., Polyn, S. M., Detre, G. J., & Haxy, J. V. (2006). Beyond mind-reading: multi-voxel pattern analysis of fMRI data. *Trends in Cognitive Sciences, 10*(9), 424–430.
Oldfield, R. C. (1971). The assessment and analysis of handedness: the Edinburgh inventory. *Neuropsychologia, 9*(1), 97–113.
Oruc, I., & Barton, J. J. S. (2011). Adaptation improves discrimination of face identity. *Proceedings of the Royal Society B, 278*, 2591–2597.
Puce, A., Allison, T., Gore, J. C., & McCarthy, G. (1995). Face-sensitive regions in human extrastriate cortex studied by functional MRI. *Journal of Neurophysiology, 74*, 1192–1199.
Regan, D. (1982). Comparison of transient and steady-state methods. *Annuals of the New York Academy of Sciences, 388*, 45–71.
Regan, D. (1989). *Human brain electrophysiology: Evoked potentials and evoked magnetic fields in science and medicine*. Elsevier.
Rhodes, G., Jeffery, L., Clifford, C. W. G., & Leopold, D. A. (2007). The timecourse of higher-level face aftereffects. *Vision Research, 47*(17), 2291–2296.
Robbins, R., & McKone, E. (2007). No face-like processing for objects-of-expertise in three behavioural tasks. *Cognition, 103*(1), 34–79.
Rolls, E. T. (2001). Representations in the brain. *Synthese, 129*, 153–171.
Rolls, E. T., Aggelopoulos, N. C., Franco, L., & Treves, A. (2004). Information encoding in the inferior temporal cortex: contributions of the firing rates and correlations between the firing of neurons. *Biological Cybernetics, 90*, 19–32.
Rossion, B. (2008). Picture-plane inversion leads to qualitative changes of face perception. *Acta Psychologica, 128*, 274–289.
Rossion, B. (2014). Understanding face perception by means of prosopagnosia and neuroimaging. *Frontiers in Bioscience, 6*, 308–317 (Elite Ed.).
Rossion, B., Alonso-Prieto, E., Boremanse, A., Kuefner, D., & Van Belle, G. (2012). A steady-state visual evoked potential approach to individual face perception: effect of inversion, contrast-reversal and temporal dynamics. *NeuroImage, 63*, 1585–1600.
Rossion, B., & Boremanse, A. (2011). Robust sensitivity to facial identity in the right human occipito-temporal cortex as revealed by steady-state visual-evoked potentials. *Journal of Vision, 11*(2), 1–21.
Rossion, B., Hanseeuw, B., & Dricot, L. (2012). Defining face perception areas in the human brain: a large-scale factorial fMRI face localizer analysis. *Brain Cognition, 79*, 138–157.
Rossion, B., & Jacques, C. (2011). The N170 : understanding the time-course of face perception in the human brain. In Luck, & E. Kappenman (Eds.), *The Oxford handbook of ERP components* (pp. 115–142). S. Oxford University Press.
Schiltz, C., & Rossion, B. (2006). Faces are represented holistically in the human occipito-temporal cortex. *NeuroImage, 32*, 1385–1394.
Schweinberger, S. R., Huddy, V., & Burton, A. M. (2004). N250r: a face-selective brain response to stimulus repetitions. *NeuroReport, 15*(9), 1501–1505.
Schweinberger, S. R., Pfütze, E. M., & Sommer, W. (1995). Repetition priming and associative priming of face recognition: evidence from event-related potentials. *Journal of Experimental Psychology – Learning, Memory, and Cognition, 21*(3), 722–736.
Schweinberger, S. R., Pickering, E. C., Jentzsch, I., Burton, A. M., & Kaufmann, J. M. (2002). Event-related brain potential evidence for a response of inferior temporal cortex to familiar face repetitions. *Cognitive Brain Research, 14*(3), 398–409.
Sergent, J. (1984). An investigation into component and configural processes underlying face perception. *British Journal of Psychology, 75*, 221–242.
Sergent, J., Ohta, S., & MacDonald, B. (1992). Functional neuroanatomy of face and object processing: a positron emission tomography study. *Brain, 115*, 15–36.
Srinivasan, R., Russell, D. P., Edelman, G. M., & Tononi, G. (1999). Increased synchronization of neuromagnetic responses during conscious perception. *Journal Neuroscience, 19*, 5435–5448.
Strobach, T., & Carbon, C. C. (2013). Face adaptation effects: reviewing the impact of adapting information, time, and transfer. *Frontiers in Perception Science, 4*, 318.
Tanaka, J. W., Curran, T., Porterfield, A. L., & Collins, D. (2006). Activation of preexisting and acquired face representations: the N250 event-related potential as an index of face familiarity. *Journal of Cognitive Neuroscience, 18*(9), 1488–1497.
Tiddeman, B. (2005). Towards realism in facial image transformation: results of a wavelet MRF method. *Computer Graphics Forum, 24*, 449–456.
Todorov, A., Pakrashi, M., & Oosterhof, N. N. (2009). Evaluating faces on trustworthiness after minimal time exposure. *Social Cognition, 27*, 813–833.
Tong, F., & Nakayama, K. (1999). Robust representations for faces: evidence from visual search. *Journal of Experimental Psychology: Human Perception and Performance, 25*, 1016–1035.
Tyler, C. W., & Kaitz, M. (1977). Movement adaptation in the visual evoked response. *Experimental Brain Research, 27*, 203–209.
Vakli, P., Németh, K., Zimmer, M., & Kovács, G. (2014). The face evoked steady-state visual potentials are sensitive to the orientation, viewpoint, expression and configuration of the stimuli. *International Journal of Psychophysiology, 94*(3), 336–350.
Valentine, T., & Bruce, V. (1986). The effect of race, inversion and encoding activity upon face recognition. *Acta Psychologica, 61*, 259–273.
Visconti di Oleggio Castello, M., Guntupalli, J. S., Yang, H., & Gobbini, M. I. (2014). Facilitated detection of social cues conveyed by familiar faces. *Frontiers in Human Neuroscience, 8*(678), 1–11.
Walter, S., Quigley, C., Andersen, S. K., & Mueller, M. M. (2012). Effects of overt and covert attention on the steady-state visual evoked potential. *Neuroscience Letters, 519*(1), 37–41.
Walther, C., Schweinberger, S. R., Kaiser, D., & Kovacs, G. (2013). Neural correlates of priming and adaptation in familiar face perception. *Cortex, 49*(7), 1963–1977.
Walther, C., Schweinberger, S. R., & Kovács, G. (2013). Adaptor identity modulates adaptation effects in familiar face identification and their neural correlates. *PLoS One, 8*(8), e70525.
Watier, N. N., & Collin, C. A. (2009). Effects of familiarity on spatial frequency thresholds for face matching. *Perception, 38*, 1497–1507.
Webster, M. A., & MacLeod, D. I. A. (2011). Visual adaptation and face perception. *Philosophical Transactions of the Royal Society of London B Biological Sciences, 366*(1571), 1702–1725.
Weiner, K. S., & Grill-Spector, K. (2010). Sparsely-distributed organization of face and limb activations in human ventral temporal cortex. *NeuroImage, 52*, 1559–1573.

Willis, J., & Todorov, A. (2006). First impressions: making up your mind after 100 ms exposure to a face. *Psychological Science, 17*, 592–598.

Winston, J. S., Henson, R. N. A., Fine-Goulden, M. R., & Dolan, R. J. (2004). fMRI-Adaptation reveals dissociable neural representations of identity and expression in face perception. *Journal of Neurophysiology, 92*(3), 1830–1839.

Xu, X., Yue, X., Lescroart, M. D., Biederman, I., & Kim, J. G. (2009). Adaptation in the fusiform face area (FFA): image or person. *Vision Research, 49*, 2800–2807.

Yin, R. K. (1969). Looking at upside-down faces. *Journal of Experimental Psychology, 81*, 141–145.

Young, A. W., Hay, D. C., McWeeny, K. H., Flude, B. M., & Ellis, A. W. (1985). Matching familiar and unfamiliar faces on internal and external features. *Perception, 14*(6), 737–746.

Young, M. P., & Yamane, S. (1992). Sparse population coding of faces in the inferotemporal cortex. *Science, 256*(5061), 1327–1331.

Yovel, G., & Kanwisher, N. (2005). The neural basis of the behavioral face-inversion effect. *Current Biology, 15*, 2256–2262.

Zhen, Z., Yang, Z., Huang, L., Kong, X., Wang, X., Dang, X., et al. (2015). Quantifying interindividual variability and asymmetry of face-selective regions: a probabilistic functional atlas. *NeuroImage, 113*, 13–25.